# Surface segregation and relaxation calculated by the embedded-atom method: Application to face-related segregation on platinum-nickel alloys

M. Lundberg
*Department of Theoretical Physics, Royal Institute of Technology, 100 44 Stockholm, Sweden*
(Received 20 May 1987)

The embedded-atom method (EAM) [M.S. Daw and M. I. Baskes, Phys. Rev. Lett. **50**, 1285 (1983); Phys. Rev. B **29**, 6443 (1984)] is applied to surface segregation and surface relaxation of binary alloys. This method needs no *ad hoc* size-mismatch strain energy and can handle arbitrary interlayer distances at the surface. Three low-index faces of platinum-nickel alloys are studied. Previously, low-energy electron diffraction investigations have established a face-related segregation on platinum-nickel alloys, with platinum enrichment on the (111) surface and nickel enrichment on the (110) surface. This work shows that EAM is capable of reproducing the experimentally determined segregation and relaxation with a good accuracy. In addition, EAM predicts the existence of a metastable concentration profile on the $Pt_{0.5}Ni_{0.5}(110)$ surface.

## I. INTRODUCTION

In the present paper the embedded-atom method[1,2] (EAM) is used to describe the energetics of atoms in substitutionally disordered binary alloys, where both multilayer segregation and multilayer relaxation are found to occur at the surface. The energy expression in the EAM is a function of atomic distances. This makes it possible to find both the composition and the geometry near the surface. A statistical approach is used to simulate the equilibrium state of the alloys.

In this work the EAM is applied to platinum-nickel alloys which show a face-related segregation[3,4] with platinum enrichment on the (111) surface and nickel enrichment on the (110) surface. The (110) surface is particularly interesting because of the large contraction of the spacing between the first and second layers. It is well known that platinum-nickel alloys are exceptions from simple segregation criteria,[5-8] which are successfully applied to a large number of other alloys. The EAM gives a quantitatively correct description of the (111) surface of platinum-nickel alloys with respect to both concentration profile and surface relaxation. For the (110) surface the EAM indicates the existence of two equilibrium states of segregation. One state is in good agreement with experiment, and the other can be interpreted as a metastable state which may be obtained by a special treatment of the crystal. It is concluded that a good description of the surface relaxation is crucial for the calculation of segregation.

The EAM is a semiempirical model, proposed by Daw and Baskes,[1,2] for the energy in a pure metal or in an alloy. This model is used in a number of different applications,[1,2,9-14] where various bulk and surface properties are studied. In a previous work Foiles[12] used Monte Carlo simulations with energies from the EAM to predict both concentrations and atomic positions for copper-nickel alloys. Surface energies and surface relaxations for pure metals[2] are obtained, and the surface reconstructions on Pt(110) (Ref. 11) and Au(100) (Ref. 14) are predicted. These results make the EAM a promising model for energies at surfaces of pure metals and alloys.

Surface segregation is of great technological importance. The properties of alloy surfaces may be completely different from the bulk properties with respect to catalytic behavior and resistance to chemical attack. A great number of works, both experimental and theoretical, deal with these phenomena.

Williams and Nason[15] use a simple bond-breaking model, where the segregation profiles are calculated from the heats of vaporization for the pure metals and the bulk activity coefficient for the alloy. They also propose a surface enthalpy relaxation, but give no recipe for the size of the relaxation. King and Donnelly[16] use an improved bond-breaking theory, where the pair potentials depend on the number of nearest neighbors. These pair potentials are obtained from the heats of vaporization, the energies of vacancy formation, and the surface energies for the pure metals. King and Donnelly use these pair energies in Monte Carlo simulations.

When the two kinds of atoms in the alloy have different radii, there is a strain in the lattice. This strain can be calculated by means of elastic continuum theory.[17] There are some drawbacks of this approach. The macroscopic elastic continuum theory may not be valid on an atomic scale and the interaction between the bond-breaking energies and the strain energies is not known. The EAM does not have these drawbacks, because the strain energies are implicit in the energy formalism.

Other approaches to surface segregation are based on tight-binding methods. Tréglia and Legrand[18] apply the common bond-breaking model with a size-mismatch energy from a simplified tight-binding approach,[19] where the strain energy in the dilute limits follows from the cohesive energy and the bulk modulus. This method is similar to the EAM, where the elastic parameters and

 

the sublimation energy are used to determine an energy function. A different tight-binding method is proposed by Mukherjee *et al.*,[20] who calculate the energy for a slab of layers from the local density of states. This is evaluated from the mixed Bethe-lattice model, which gives the density of states for an atom embedded in an effective medium.

This paper is organized as follows. Section II describes the EAM and the statistical theory for bulk and surface properties. Section III presents calculations of segregation and relaxation profiles for five platinum-nickel alloys. The application of EAM to surface segregation is discussed in Sec. IV, and in Sec. V the conclusions drawn from this work are presented.

## II. THEORY

### A. Embedded-atom method

In EAM, the total electron energy is written as a superposition of contributions from individual atoms. The energy contribution from a single atom is in principle a functional of the electron density arising from the other atoms.[21] In EAM the electron density is approximated by a uniform electron density calculated from superpositions of atomic electron densities. A uniform electron density is a crude approximation, but can be improved by adding the core-core interaction. The total energy is then written

$$E_{\rm tot}=\sum_i F[\rho_h(\mathbf{r}_i),Z_i]+\tfrac{1}{2}\sum_{\substack{i,j\\(i\neq j)}}\phi(R_{ij},Z_i,Z_j)\ , \tag{1}$$

where $i$ and $j$ are subscripts enumerating all the atoms of the solid. The $i$th atom is supposed to sit at position $\mathbf{r}_i$ and to have the atomic number $Z_i$. $\rho_h(\mathbf{r}_i)$ is the electron density of the host of atoms surrounding the $i$th atom, and the function $F[\rho_h(\mathbf{r}_i),Z_i]$ gives the energy to embed the $i$th atom in the host. $\phi(R_{ij},Z_i,Z_j)$ is the repulsive core-core interaction between two atoms with atomic numbers $Z_i$ and $Z_j$ and separation $R_{ij}=|\mathbf{r}_i-\mathbf{r}_j|$. The EAM is discussed by Manninen,[22] who concludes that expression (1) can be derived formally as an approximation of the density-functional theory.

The next step is to find the functions $F$ and $\phi$ in Eq. (1). The core-core terms $\phi(R,Z_i,Z_j)$ are written as screened Coulombic potentials,

$$\phi(R,Z_i,Z_j)=\frac{C(R,Z_i)C(R,Z_j)}{R}\ , \tag{2}$$

$$C(R,Z)=C_0(Z)[1+\beta(Z)R^{\nu(Z)}]e^{-\alpha(Z)R}\ . \tag{3}$$

$C_0$ is taken to be the number of outer electrons and $\alpha$, $\beta$, and $\nu$ are fitted to experimental data. In connection with alloys, the embedding function $F[\rho_h(\mathbf{r}_i),Z_i]$ must be available for electron densities different from the pure metal densities. The effect of variations of the electron density can be obtained from the sublimation energy versus the lattice parameter. First-principles calculations and compressibility experiments of metals[23] show that the sublimation energy versus the lattice parameter $a$, $E(a)$, can be approximated by

$$E(a)=E_{\rm sub}^{\rm eq}(1+a^*)\exp(-a^*)\ , \tag{4}$$

$$a^*=\left[\frac{a}{a_0}-1\right]\left[\frac{9B\Omega}{-E_{\rm sub}^{\rm eq}}\right]^{1/2}\ . \tag{5}$$

Here $E_{\rm sub}^{\rm eq}$ is the sublimation energy at the equilibrium lattice parameter $a_0$, $B$ is the bulk modulus, and $\Omega$ is the equilibrium volume per atom. In the present work, as in Refs. 1 and 2, the superposition of atomic orbitals from the tables of atomic data in Refs. 24 and 25 is used.

The tables of atomic data have to be used with care. The number of outer $s$ and $d$ electrons is different when the atoms compose a solid and when they are free. We can take this difference into account by introducing another parameter $n_s$, giving the number of outer $s$ electrons of an atom in the alloy. If the total number of outer electrons is $N_a$, the electron density at radius $R$ from an ion core of atomic number $Z_i$ is given by

$$\rho_a(R,Z_i)=n_s\rho_a^s(R,Z_i)+(N_a-n_s)\rho_a^d(R,Z_i)\ , \tag{6}$$

where the electron densities $\rho_a^s$ and $\rho_a^d$ refer to the outer $s$ and $d$ orbitals of a free atom. The electron density of the host of atoms surrounding position $i$ then follows from the sum

$$\rho_h(\mathbf{r}_i)=\sum_{\substack{j\\(j\neq i)}}\rho_a(R_{ij},Z_j)\ . \tag{7}$$

The four parameters $\alpha$, $\beta$, $\nu$, and $n_s$ in expressions (1)–(7) determine the embedding function $F[\rho_h(\mathbf{r}_i),Z_i]$. We utilize the parameters published by Foiles *et al.*[2] These workers fitted $\alpha$, $\beta$, $\nu$, and $n_s$ for copper, silver, gold, nickel, palladium, and platinum to the elastic properties, lattice constants, vacancy formation, and sublimation energies for the pure metals, and at the same time, to the heat of solution for the binary alloys in the dilute limits. This approach gives proper embedding functions and core-core interactions for the binary alloys as well as for the pure metals.

### B. Bulk properties

The energy calculated from the EAM can be used to predict the equilibrium state of alloys. In his work on copper-nickel alloys, Foiles[12] makes a rearrangement of the atoms by a Monte Carlo simulation to find an equilibrium composition. In this work we use a statistical approach, where any atom is studied in an average environment. We consider a disordered alloy $A_xB_{1-x}$, where an atom $A$ occurs with the probability $x$ and an atom $B$ with the probability $1-x$. In contexts where $Z_i$ signifies the atomic number of species $A$ (species $B$), the letter $A$ ($B$) is used instead of $Z_i$ in $\rho_a$ and $\phi$. The averaged host electron density follows from

$$\rho_h(\mathbf{r}_i)=\sum_{\substack{j\\(j\neq i)}}[x\rho_a(R_{ij},A)+(1-x)\rho_a(R_{ij},B)]\ . \tag{8}$$

This expression is independent of $i$, if we assume translational invariance in the solid. For the core-core interaction we have two possibilities depending on the type of the randomly chosen atom. The energy equals, for an

atom $A$ at position $i$,

$$E_{A,i}(x)=F[\rho_h(\mathbf{r}_i),A]+\tfrac{1}{2}\sum_{\substack{j\\(j\neq i)}}[x\phi(R_{ij},A,A)+(1-x)\phi(B_{ij},A,B)] \tag{9}$$

and, for an atom $B$ at position $i$,

$$E_{B,i}(x)=F[\rho_h(\mathbf{r}_i),B]+\tfrac{1}{2}\sum_{\substack{j\\(i\neq j)}}[x\phi(R_{ij},B,A)+(1-x)\phi(R_{ij},B,B)] . \tag{10}$$

Since Eqs. (9) and (10) are independent of $i$ with translational invariance in the solid, we can drop the label $i$ and write $E_A(x)$ and $E_B(x)$. We now calculate the energy for an average atom in the alloy as

$$E(x)=xE_A(x)+(1-x)E_B(x) . \tag{11}$$

The heat of solution $\Delta H$ can be calculated from

$$\Delta H(x)=E(x)+xE^A_{\text{sub}}+(1-x)E^B_{\text{sub}} , \tag{12}$$

where $E^A_{\text{sub}}$ and $E^B_{\text{sub}}$ are sublimation energies for $A$ and $B$, respectively. Table I shows an example of calculated heats of solution. The good agreement with the experimental values[26] is not surprising since the parameters used to describe the energies were fitted to the dilute limits of the heats of solution.

### C. Surfaces of alloys

The surface can be considered as a slab of $N$ atomic layers, the compositions of which are to be optimized with the boundary condition that the composition of the bulk layers is fixed. The energy in the surface slab can be calculated in the same way as in the bulk, given the layer dependence of the concentration. In this model the energy is a function of $N$ concentrations, $E=E(x_1,x_2,\ldots,x_N)$ where $x_k$ is the concentration of atom $A$ in layer $k$, $k=1,2,\ldots,N$. We now apply classical thermodynamics and write the free energy $G$ for the slab[15]

TABLE I. Comparison between calculated and experimental[26] heats of solution for $Pt_xNi_{1-x}$.

| Concentration ($x$) | Heats of solution (cal/mol) Theory | Experiment |
|---|---|---|
| 0.10 | −671 | −651 |
| 0.20 | −1266 | −1340 |
| 0.30 | −1674 | −1867 |
| 0.40 | −1876 | −2146 |
| 0.50 | −1889 | −2214 |
| 0.60 | −1724 | −2159 |
| 0.70 | −1402 | −1730 |
| 0.80 | −1019 | −1225 |
| 0.90 | −475 | −762 |

$$G=E(x_1,x_2,\ldots,x_N)+k_BT\sum_{k=1}^{N}[x_k\ln x_k+(1-x_k)\ln(1-x_k)] , \tag{13}$$

assuming that the substitutional disorder can be represented sufficiently well by the configurational entropy. $T$ is the temperature and $k_B$ is Boltzmann's constant. We find the equilibrium concentrations by minimizing the free energy with respect to $x_k$ with the constraint that the total number of $A$ atoms (i.e., $\sum_k x_k$) is a constant. Introducing a Lagrange multiplier $\mu$ to remove the constraint, we search for the stationary points of the function

$$G(x_1,x_2,\ldots,x_N)-\mu\sum_{k=1}^{N}x_k . \tag{14}$$

This gives

$$\frac{\partial E}{\partial x_k}+k_BT\ln\left[\frac{x_k}{1-x_k}\right]=\mu,\quad k=1,2,\ldots,N . \tag{15}$$

The chemical potential $\mu$ is the same for all layers. It can be calculated for a layer $b$ well inside the bulk, where the concentration is known:

$$\frac{\partial E}{\partial x_b}+k_BT\ln\left[\frac{x_b}{1-x_b}\right]=\mu . \tag{16}$$

From Eqs. (15) and (16) we get the system of equations

$$\frac{x_k}{1-x_k}=\frac{x_b}{1-x_b}\exp\left[\frac{1}{k_BT}\left[\frac{\partial E}{\partial x_b}-\frac{\partial E}{\partial x_k}\right]\right],\quad k=1,2,\ldots,n . \tag{17}$$

These equations give the concentration profile of the alloy.

## III. CALCULATIONS

### A. Calculation of surface relaxations

In principle, the relaxation of the interlayer distances near the surface can be obtained by minimizing the free energy with respect to the interlayer distances. This must be done with some care to get reliable results. The problem is that the total number of atoms of a given kind does not come out exactly constant in Eq. (17), unless the concentration profile gradually approaches and attains the concentration $x_b$ in the $N$th layer. The energy is more sensitive to this artificial change in the number of atoms than to the relaxation. If the optimization of the relaxation and the composition is made simultaneously, the result will be in poor agreement with experiment.

We have found two ways to overcome this problem. In Eq. (17) a $(N+1)$th layer can be introduced with a concentration $x_{N+1}$ chosen so as to give a concentration profile $x_k$, $k=1,2,\ldots,N+1$, an average value equal to the bulk concentration $x_b$. Another way to calculate the relaxation is to optimize the relaxation for fixed concen-

TABLE II. Iteration scheme for calculating compositional profile and relaxation. $x_k^{Pt}$, $k=1,2,3,4$, is the platinum concentration of layer $k$. $\Delta_{12}$ and $\Delta_{23}$ give the spacings between the first and second layer and between the second and third layer, respectively. Positive (negative) values of $\Delta_{12}$ and $\Delta_{23}$ signify expansion (contraction). The first iteration of $x_k^{Pt}$ conveniently starts from $\Delta_{12}=\Delta_{23}=0$.

| Iteration | $\Delta_{12}$ (%) | $\Delta_{23}$ | $x_1^{Pt}$ | $x_2^{Pt}$ | $x_3^{Pt}$ (at. %) | $x_4^{Pt}$ |
|---|---|---|---|---|---|---|
| 0 | 0.0 | 0.0 | | | | |
| 1 | | | 66.0 | 47.9 | 51.0 | 49.6 |
| 2 | −2.7 | 0.9 | | | | |
| 3 | | | 64.0 | 42.0 | 54.4 | 48.3 |
| 4 | −3.9 | 0.3 | | | | |
| 5 | | | 65.1 | 37.8 | 55.5 | 47.9 |
| 6 | −4.5 | −0.2 | | | | |
| 7 | | | 65.8 | 35.0 | 55.9 | 47.8 |
| 8 | −5.0 | −0.7 | | | | |
| 9 | | | 66.7 | 32.6 | 56.3 | 47.7 |
| 10 | −5.2 | −1.1 | | | | |
| 11 | | | 67.2 | 31.3 | 56.4 | 47.6 |
| 12 | −5.3 | −1.3 | | | | |
| 13 | | | 67.5 | 30.6 | 56.4 | 47.6 |
| 14 | −5.3 | −1.4 | | | | |

trations and, separately, the concentrations for fixed relaxation. The scheme can be iterated to a result in qualitative agreement with experiment. An example of this procedure is given in Table II. The relaxations are rather insensitive to the concentrations and seem to converge to a unique geometry. The two methods give similar results. In the rest of the paper the latter approach is chosen.

### B. Dependence on the number of optimized layers

If the concentrations in the three surface layers are sought, it is enough to optimize four layers in Eq. (17). More layers will change the concentrations in the three outermost layers by the order of 1 at. %. The relaxation of the two outermost interlayer distances is changed a few tenth of a percent when the number of optimized layers is increased from four to seven. However, for the (110) and (100) surfaces the calculated concentrations of layers far from the surface behave in a strange way. For the $Pt_{0.5}Ni_{0.5}$ (110) and (100) surfaces we obtain platinum concentrations alternating between 4 and 96 at. % far from the surface. These oscillations are not damped when the number of optimized layers is increased. This may indicate a fundamental problem with the model or a strong tendency for the alloy to order in a region of several layers near the surface.

### C. Multiple solutions to the segregation equation

An interesting fact is that Eq. (17) does not always give a unique solution $x_k$, $k=1,2,\ldots,N$. Hence, if the task is to find *all* solutions to Eq. (17), an iterative procedure is disqualified, since, in general, the way its start influences its end is unknown. A straightforward method to determine unique or multiple solutions to Eq. (17) is the following. For a limited number of layers $N$, one sets up a grid of concentrations filling the $N$-dimensional cube formed by $x_k$, $k=1,2,\ldots,N$, running from 0 to 100 at. %, and for each point of the grid one calculates the right-hand member of Eq. (17). If the value is sufficiently close to the left-hand member, the considered concentrations $x_k$ are near to a solution of Eq. (17). We have carried through calculations of this kind for $N=3$. For the (111) and (100) surfaces just one solution is found. For the (110) surface Eq. (17) gives a more complicated behavior, as illustrated in Fig. 1 for the outermost layer. The result is striking, as one finds three solutions to Eq. (17) for a range of bulk concentrations. The dotted line in the middle indicates saddle points and the two solid lines correspond to true local minima.

An iterative method of solving Eq. (17) always converges to one of the solid-line solutions, and provided

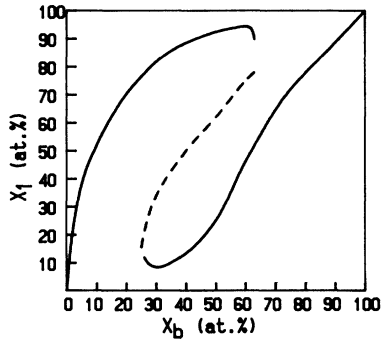


FIG. 1. Platinum concentration in the first layer, $x_1$, vs platinum concentration in the bulk, $x_b$. The solid lines are local mimima in the free energy, and the dotted line represents saddle points. The interlayer distance between the first and second layer is contracted 10%, and the temperature is 1200 K.

the iterations start sufficiently near one of the solutions, the procedure will converge to this one. On the other hand, an iterative procedure fails to hit the dotted-line solutions. In the calculation illustrated in Fig. 1 the spacing between the first and second layer is contracted 10% in relation to the spacing of the (110) layers in the bulk. Test calculations show that the threefold solution to Eq. (17) exists for all reasonable spacings between the first and second layer, although the range of bulk concentrations where multiple solutions are found may change. Figure 2 shows the free energy as a function of the concentrations in layers 1 and 2 for $Pt_{0.5}Ni_{0.5}(110)$. The concentration $x_3$ is chosen so as to give the correct averaged concentration over three layers. It is instructive to see the two minima and the saddle point. When the bulk concentration is changed, the saddle point approaches one of the minima and for a certain bulk concentration one of the minima disappears and the solution becomes unique.

The enrichment of nickel in the top layer (lower solid curve in Fig. 1) will be considered as a stable segregation state, and the enrichment of platinum in the top layer (upper solid curve in Fig. 1) will be considered as a metastable segregation state. Since the EAM gives a qualitatively correct description of three (111) surfaces, and since one of the calculated concentration profiles of $Pt_{0.5}Ni_{0.5}(110)$ is in excellent agreement with experiment (Sec. III D), we have reason to believe that the prediction of a metastable state on the (110) surfaces is correct. This metastable state should be available under special experimental conditions. One must keep in mind that the platinum-rich state may be reconstructed as in the case of pure platinum (110).[27] The method of calculation used in the present work can be adapted for reconstructed surfaces.[11]

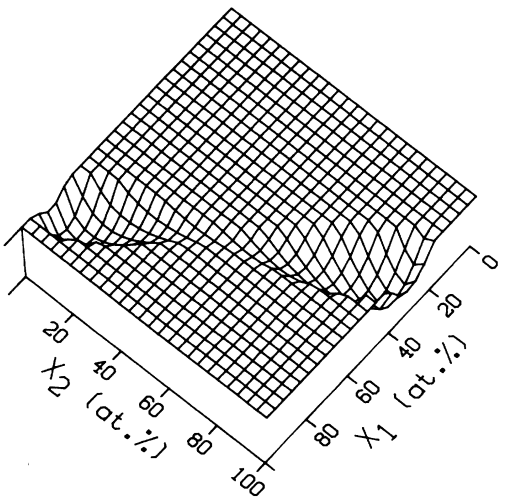


FIG. 2. Free energy vs platinum concentrations $x_1$ and $x_2$ in first and second layers for $Pt_{0.5}Ni_{0.5}(110)$. The interlayer distances and temperature are the same as in Fig. 1. The energy is in arbitrary units.

### D. Results

Experimental composition profiles and relaxations are available from low-energy electron diffraction (LEED) for the (111) surfaces[3] of $Pt_{0.1}Ni_{0.9}$, $Pt_{0.5}Ni_{0.5}$, and $Pt_{0.78}Ni_{0.22}$, and the (110) surface[4] of $Pt_{0.5}Ni_{0.5}$. The top-layer concentrations determined by LEED for the (111) surfaces are in excellent agreement with the results obtained by ion scattering spectroscopy and Auger-electron spectroscopy.[28] The LEED measurements, listed in Table III, show that face-related segregation occurs at the low-index surfaces of platinum-nickel alloys. With 50-at. % Pt the (111) surface segregates with platinum in the topmost layer, while the (110) surface segregates with nickel in the topmost layer. In both cases there is an oscillatory concentration profile, whose amplitude is more pronounced for the (110) surface. For the (111) surfaces the relaxation is small, while the relaxation for the (110) surface exhibits a strong oscillation with 19% contraction between the first and second layer and 10% expansion between the second and third layer.

Theoretical composition profiles corresponding to 1200 K are compared with experimental profiles in Table III. Interlayer spacings for three different cases are used in the calculation: a nonrelaxed surface, a surface with relaxation determined by LEED investigations, and finally, a relaxation obtained by optimization of the energy as discussed in Sec. III A.

The calculated segregation for the (111) surfaces agrees convincingly well with the experimentally determined top-layer segregation for any of the aforementioned relaxation models. The nickel-rich $Pt_{0.1}Ni_{0.9}(111)$ alloy is a case where the calculation is in almost perfect agreement with respect to both segregation and relaxation. For $Pt_{0.5}Ni_{0.5}(111)$ and $Pt_{0.78}Ni_{0.22}(111)$ the optimized spacing between the first and second layer are contracted 5% instead of 1%, and the segregation is too weak in all layers. The segregation in the top layer turns out to be rather insensitive to relaxation, but the compositional oscillations become stronger with an optimized relaxation than with no relaxation.

For $Pt_{0.5}Ni_{0.5}(110)$, two different solutions to Eq. (17) are obtained (See Sec. III C). One solution is in very good agreement with the experiment and is called a stable segregation state in Table III. The calculated relaxation between the first and second layer is 14% contraction instead of 19% contraction in the LEED study. The calculated relaxation between the second and third layer is close to zero instead of 10% expansion found by LEED. The concentration profile agrees closely with the experiment when the interlayer spacings are taken from the experiment, and it is fairly correct when the relaxation is calculated. However, if an unrelaxed surface is assumed, hardly any nickel enrichment results. We conclude that a model which permits a realistic geometry is crucial for the (110) surface.

## IV. DISCUSSION

### A. The EAM calculations

The EAM has previously been used in a Monte Carlo simulation of surface segregation.[12] The difference be-

tween a Monte Carlo simulation and a mean-field approach was investigated by King and Donnelly.[16] They made an interesting comparison between the segregation profiles produced by Monte Carlo simulation and those resulting from the model of Williams and Nason.[15] The obtained segregation profiles are very close for gold-silver alloys, when the same description of the pair energies is used in both cases. By analogy we believe that the thermodynamical Eq. (17) is equally well suited for obtaining the segregation as Monte Carlo simulation, at least when we do not wish to, study finer details of the alloy composition as, for instance, clustering in layers.

It is interesting to apply the EAM together with the parameters published by Foiles *et al.*[2] to pure platinum, pure nickel, and platinum-nickel alloys and to compare the calculated relaxations.

TABLE III. Concentration profiles and relaxations for platinum-nickel alloys. The values obtained from the EAM are compared with experimental values (Refs. 3 and 4) and with tight-binding results (Ref. 18). Three different choices for the interlayer spacings are used: a nonrelaxed surface, a surface with relaxation determined by LEED, and finally, a relaxation obtained by optimization of the energy as explained in Sec. III A. The relaxations are given in percent and the concentrations in atomic percent.

| | No relaxation | EAM Relaxation from LEED | Calculated relaxation | LEED study[a] | Tight-binding[b] |
|---|---|---|---|---|---|
| | | | $Pt_{0.1}Ni_{0.9}(111)$ | | |
| $x_1^{Pt}$ | 27 | 27 | 27 | 30 | 23 |
| $x_2^{Pt}$ | 5 | 5 | 5 | 5 | 7 |
| $x_3^{Pt}$ | 12 | 11 | 12 | 10 | 10 |
| $\Delta_{12}$ | 0 | 0.0 | −0.7 | 0.0 | |
| $\Delta_{23}$ | 0 | 0.8 | 0.2 | 0.8 | |
| | | | $Pt_{0.5}Ni_{0.5}(111)$ | | |
| $x_1^{Pt}$ | 66 | 66 | 68 | 88 | 70 |
| $x_2^{Pt}$ | 48 | 41 | 31 | 9 | 43 |
| $x_3^{Pt}$ | 52 | 49 | 56 | 65 | 52 |
| $\Delta_{12}$ | 0 | −1.0 | −5.3 | −1.0 | |
| $\Delta_{23}$ | 0 | −2.4 | −1.4 | −2.4 | |
| | | | $Pt_{0.78}Ni_{0.22}(111)$ | | |
| $x_1^{Pt}$ | 90 | 90 | 87 | 99 | 90 |
| $x_2^{Pt}$ | 80 | 73 | 72 | 30 | 73 |
| $x_3^{Pt}$ | 77 | 76 | 82 | 87 | 82 |
| $\Delta_{12}$ | 0 | −2 | −4.7 | −2 | |
| $\Delta_{23}$ | 0 | −2 | −0.9 | −2 | |
| | | | $Pt_{0.5}Ni_{0.5}(110)$ stable state | | |
| $x_1^{Pt}$ | 39 | 13 | 25 | 0 | 62 |
| $x_2^{Pt}$ | 97 | 98 | 95 | 95 | 60 |
| $x_3^{Pt}$ | 5 | 10 | 2 | 17 | 39 |
| $\Delta_{12}$ | 0 | −19 | −14 | −19 | |
| $\Delta_{23}$ | 0 | 10 | 0 | 10 | |
| | | | $Pt_{0.5}Ni_{0.5}(110)$ metastable state[c] | | |
| $x_1^{Pt}$ | | 91 | 91 | 0 | 62 |
| $x_2^{Pt}$ | | 3 | 0 | 95 | 60 |
| $x_3^{Pt}$ | | 95 | 90 | 17 | 39 |
| $\Delta_{12}$ | | −19 | −14 | −19 | |
| $\Delta_{23}$ | | 10 | 1 | 10 | |
| | | | $Pt_{0.5}Ni_{0.5}(100)$ | | |
| $x_1^{Pt}$ | 90 | | 93 | | 75 |
| $x_2^{Pt}$ | 14 | | 0 | | 34 |
| $x_3^{Pt}$ | 84 | | 87 | | 57 |
| $\Delta_{12}$ | 0 | | −11.6 | | |
| $\Delta_{23}$ | 0 | | −4.2 | | |

[a]References 3 and 4.
[b]Reference 18.
[c]No metastable state is predicted with the unrelaxed geometry.

Let us first consider the (111) surface of Pt, Ni, and Pt-Ni alloys. The relaxation between the first and second layer for Pt(111) is 5% contraction according to the theory[2] and 1% expansion according to the experiment.[29] For Ni(111) a calculation[2] gives no relaxation against 1% contraction for the experiment.[30] This means that the EAM gives a relaxation which is 6% too small for Pt(111) and 1% too large for Ni(111). For a nickel-rich alloy surface we then expect that a calculation of the relaxation would be almost correct. In fact, the optimized relaxation turns out to be 1% too small compared with the experimental relaxation[3] for the $Pt_{0.1}Ni_{0.9}(111)$, which has 70% nickel at the surface. For a platinum-rich alloy we expect the calculated relaxation to be around 5% too small. The calculated value is found to be 4% too small for $Pt_{0.5}Ni_{0.5}(111)$ and 3% too small for $Pt_{0.78}Ni_{0.22}(111)$.

We now turn our attention to the (110) surface of pure Ni and the $Pt_{0.5}Ni_{0.5}$ alloy. For the (110) surface of pure nickel the EAM predicts[2] 2% contraction, while the experiment[31] gives 8% contraction. We thus expect a relaxation which is 6% too large in the calculation, if the first layer is a complete nickel layer. The EAM in fact predicts a 5% too large relaxation for $Pt_{0.5}Ni_{0.5}(110)$.

The disagreement between the calculated and the measured relaxations as discussed in the two last paragraphs shows a systematic trend. The disagreement in the relaxations for the alloys turns out to be rather close to the disagreement found for the pure metals constituting the alloys. It must be kept in mind that in the present version of the EAM only bulk properties are used for determining the parameters of the material. If surface properties were introduced in the EAM in a way that gave accurate relaxations for the pure metals, we could expect an agreement within maybe 1% for the relaxation between the first and second layer of the alloys.

### B. Other theoretical models

The segregating element for most alloys can be predicted by qualitative criteria for polycrystalline and dilute alloys. Platinum-nickel is one of the very few systems where such criteria fail. Miedema suggested a model which can explain 21 out of the 22 studied systems.[5] Abraham and Brundle tested another model against 45 alloy systems, where 38 predictions were correct.[6] Chelikowsky suggested a criterion which can explain 35 out of 40 studied systems.[7] Mezey and Giber presented an approach which gives the correct behavior for 39 out of the 40 systems.[8] Abraham and Brundle got neither solvent nor solute segregation for dilute nickel in platinum, and in the three other works the authors got nickel segregation instead of platinum segregation. The qualitative segregation criteria are designed for polycrystalline samples with an averaged surface structure very similar to an actual (111) surface, but, nevertheless, they fail to predict the segregation on the (111) surface of $Pt_{0.1}Ni_{0.9}$ and $Pt_{0.78}Ni_{0.22}$.

The commonly used bond-breaking model,[17] without any size-mismatch corrections, fails to predict platinum segregation for the (111) surfaces of platinum. This model predicts 2 and 61 at. % platinum in the toplayer at 1000 K (30 and 99 at. % according to experiment) for $Pt_{0.1}Ni_{0.9}(111)$ and $Pt_{0.78}Ni_{0.22}(111)$, respectively. The size mismatch can be included in the bond-breaking model by elastic continuum theory as in Ref. 17. This approach gives 16 and 33 at. % platinum in the top layer at 1000 K for $Pt_{0.1}Ni_{0.9}(111)$ and $Pt_{0.78}Ni_{0.22}(111)$, respectively. The nickel-rich alloy is reasonably well described with the elastic strain term, while the platinum-rich alloy is poorly described. The conclusion is that these simple theories are inapplicable to platinum-nickel alloys.

Gijzeman[32] assumed Lennard-Jones potentials for the energy versus the nearest-neighbor distance. This method gives a modification of the pair-bonding energies, when the lattice parameter is different from those of the pure metals. The prediction of the segregation nevertheless disagrees with the experiment, since nickel segregation results for the (111) surfaces.

Tréglia and Legrand[18] used a tight-binding approach to impurities for calculating the size-mismatch energy. The mismatch energies for the dilute alloys were then interpolated for nondilute bulk concentrations and added to the usual bond-breaking energy. For the (111) surface they obtained the same concentration profiles as in this work within a few percent, but for the (110) surface they predicted platinum segregation, in disagreement with LEED experiments and with this work (Table III).

As far as we know the EAM is hitherto the only approach that is able to describe quantitatively the segregation on both the (111) and (110) surfaces of platinum-nickel systems.

## V. CONCLUSIONS

The EAM offers a promising approach to the energetics of surface segregation. Unlike pair-bonding models, the EAM is not limited to nearest-neighbor interactions. The atomic-size-mismatch effect is intrinsic in the EAM and no *ad hoc* mismatch energies have to be added. The model also permits lattice relaxation and surface reconstruction.

For platinum-nickel alloys the face-related segregation occurring on the low-index surfaces is reproduced by the EAM. The calculated relaxations are in qualitative agreement with available LEED measurements. A realistic choice of interlayer distances at the surface is crucial for obtaining a correct concentration profile. The EAM predicts a metastable concentration profile for the (110) surface for platinum concentrations between 20 and 60 % in the bulk.

## ACKNOWLEDGMENT

Discussions with Dr. J. Rundgren are gratefully acknowledged.

[1]M. S. Daw and M. I. Baskes, Phys. Rev. Lett. **50**, 1285 (1983); Phys. Rev. B **29**, 6443 (1984).
[2]S. M. Foiles, M. I. Baskes, and M. S. Daw, Phys. Rev. B **33**, 7983 (1986).
[3]Y. Gauthier, Y. Joly, R. Baudoing, and J. Rundgren, Phys. Rev. B **31**, 6216 (1985); R. Baudoing, Y. Gauthier, M. Lundberg, and J. Rundgren, J. Phys. C **19**, 2825 (1986).
[4]Y. Gauthier, R. Baudoing, M. Lundberg, and J. Rundgren, Phys. Rev. B **35**, 7867 (1987).
[5]A. R. Miedema, Z. Metallk. **69**, 455 (1978).
[6]F. F. Abraham and C. R. Brundle, J. Vac. Sci. Technol. **18**, 506 (1981).
[7]J. R. Chelikowsky, Surf. Sci. Lett. **139**, L197 (1984).
[8]L. Z. Mezey and J. Giber, Surf. Sci. **162**, 514 (1985).
[9]M. S. Daw and R. L. Hatcher, Solid State Commun. **56**, 697 (1985).
[10]S. M. Foiles, Phys. Rev. B **32**, 3409 (1985).
[11]M. S. Daw, Surf. Sci. Lett. **166**, L161 (1986).
[12]S. M. Foiles, Phys. Rev. B **32**, 7685 (1985).
[13]S. M. Foiles and M. S. Daw, J. Vac. Sci. Technol. A **3**, 1565 (1985).
[14]B. W. Dodson, Phys. Rev. B **35**, 880 (1987).
[15]F. L. Williams and D. Nason, Surf. Sci. **45**, 377 (1974).
[16]T. S. King and R. G. Donnelly, Surf. Sci. **74**, 89 (1978); Surf. Sci. **141**, 417 (1984).
[17]P. Wynblatt and R. C. Ku, Surf. Sci. **65**, 511 (1977).
[18]G. Tréglia and B. Legrand, Phys. Rev. B **35**, 4338 (1987).
[19]D. Tománek, A. A. Aligia, and C. A. Balseiro, Phys. Rev. B **32**, 5051 (1985).
[20]S. Mukherjee, J. L. Morán-López, V. Kumar, and K. H. Bennemann, Phys. Rev. B **25**, 730 (1982).
[21]M. J. Scott and E. Zaremba, Phys. Rev. B **22**, 1564 (1980).
[22]M. Manninen, Phys. Rev. B **34**, 8486 (1986).
[23]J. H. Rose, J. R. Smith, F. Guinea, and J. Ferrante, Phys. Rev. B **29**, 2963 (1984).
[24]E. Clementi and C. Roetti, At. Data Nucl. Data Tables **14**, 177 (1974).
[25]A. D. McLean and R. S. McLean, At. Data Nucl. Data Tables **26**, 197 (1981).
[26]R. Hultgren, P. D. Desai, D. T. Hawkins, M. Gleiser, and K. K. Kelly, *Selected Values of the Thermodynamic Properties of Binary Alloys* (American Society for Metals, Metals Park, OH, 1973).
[27]D. L. Adams, H. B. Nielsen, M. A. Van Hove, and A. Ignatiev, Surf. Sci. **104**, 47 (1981).
[28]J. C. Bertolini, J. Massardier, P. Delichere, B. Tardy, B. Imelik, Y. Jugnet, Tran Minh Duc, L. De Temmerman, C. Creemers, H. Van Hove, and A. Neyens, Surf. Sci. **119**, 95 (1982); L. De Temmerman, C. Creemers, H. Van Hove, A. Neyens, J. C. Bertolini, and J. Massardier, Surf. Sci. **178**, 888 (1986).
[29]D. L. Adams, H. B. Nielsen, and M. A. Van Hove, Phys. Rev. B **20**, 4789 (1979).
[30]J. E. Demuth, P. M. Marcus, and D. W. Jepsen, Phys. Rev. B **11**, 1460 (1975).
[31]Y. Gauthier, R. Baudoing, Y. Joly, C. Gaubert, and J. Rundgren, J. Phys. C **17**, 4547 (1984).
[32]O. L. J. Gijzeman, Surf. Sci. **150**, 1 (1985).